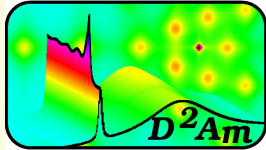


# 2D detectors and application of XPAD pixel detector in material sciences : powder and multilayers.

J.-F. Bérar, S. Arnaud, S. Basolo, N. Boudet, P. Breugnon, B. Caillot, J.-C. Clemens, P. Delpierre, B. Dinkepiler, S. Hustache, I. Koudobine, M. Menouni, H. Pallancher, P. Pangaud, R. Potheau, E. Vigeolas



D2AM/CRG-ESRF  
Grenoble



LdC-CNRS



SOLEIL  
St Aubin



CPPM-IN2P3-CNRS  
Marseille

Feb. 20th, 2006



Campinas sincrotron

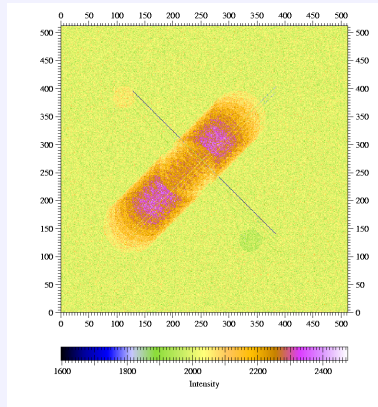
# Summary.

- Synchrotron experiments images. 3
- XPAD project and prototypes 11
- Resolution, dynamical range, . . . 14
- Kinetics potentiality 17
- Powder diffraction application 20
- Multilayer studies 27
- CCD compared to hybrid pixels 29

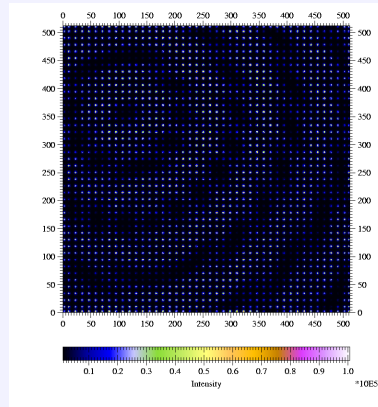
# Synchrotron experiments images.

"Experimental" images seen on similar scales for :

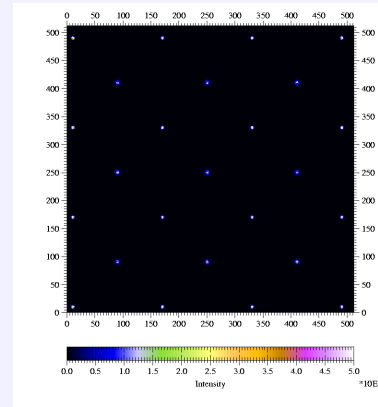
Absorption



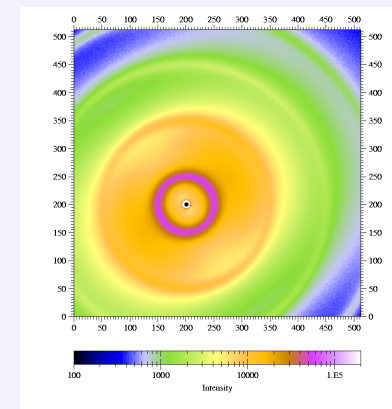
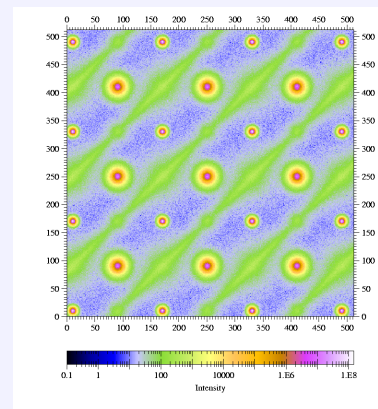
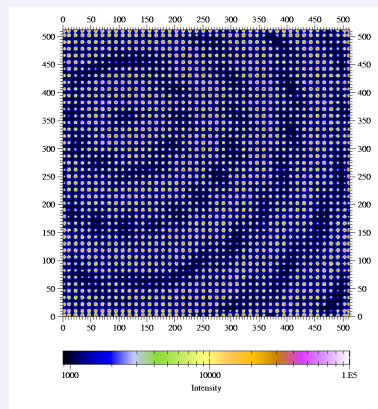
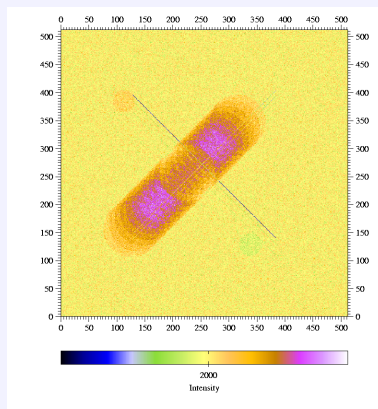
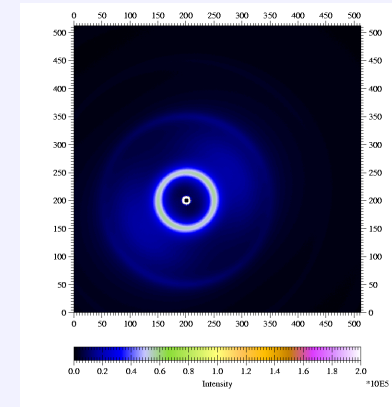
Struct. Cryst.



Material Science



SAXS

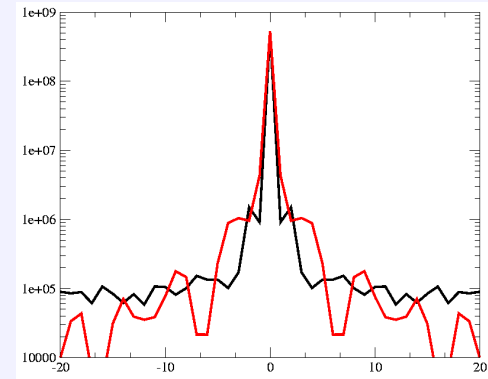
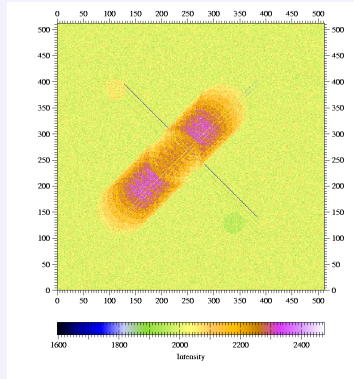


LINEAR or LOG scaled views show that requirements are very different between experiments.

# Absorption images.

Evidence weakly contrasted details using the weakest radiation dose.

In Fourier transform, significative magnitudes near origine :



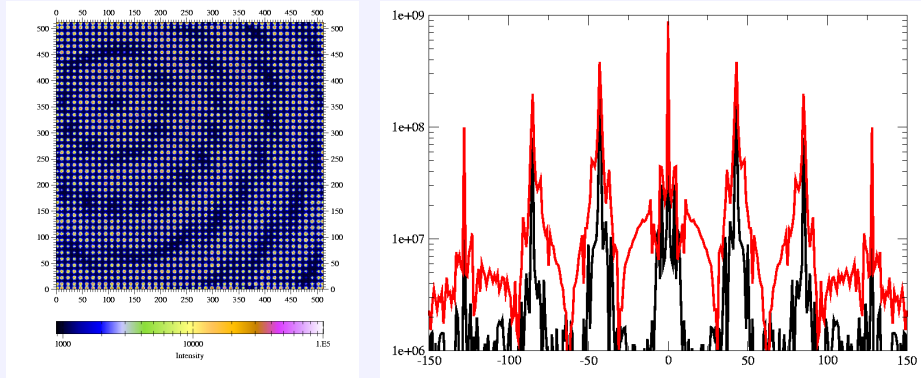
- small details  $\Rightarrow$  expected resolution  $50\mu m$
- $\Delta \approx 0.01 > \sigma \Rightarrow$  counts  $\gg 10^4 \Rightarrow$  14-16 bits
- operate at high energy (80 keV) : high Z sensor needed (GaAs)

**MEDIPIX (CERN)** *Llopart, IEEE-TNS 2002*, **MPEC (Bonn)** *Lindner, NIM 2000*



# Structure collection (PX).

Structure collection : **integrate quickly** the maximum number of peaks.



- counts range :  $\approx 10^3$  (diffuse) -  $\approx 10^6$   
 $\Rightarrow$  18-20 bits useful
- pixel size  $< \approx$  beam spot size  $\approx 100\mu m$
- energy range : 10 - 25 keV

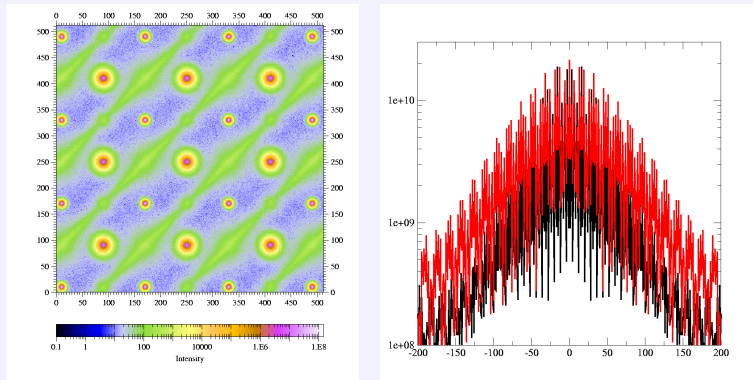
- integration (5 pixels) over background  $\Rightarrow$  at less 25 pixels/peak
- very big surface : a few  $10^6$  pixels required
- detector motion are restricted :  $2\theta_{center} < \approx 10^\circ$

**PILATUS (PSI)** Brönninmann, JSR 2002, PSI 2005

# Material Science or Solid state physics

Exploration of reciprocal space, profile shape, diffuse scattering...

The Fourier transform of the image is widely spread.



- 5 keV - 25 keV
  - 1 to  $10^9$  photons/s (BM2)
- ⇒ 32 bits usefull

- resolution optimized during experiment by adjusting detector position

⇒ pixel size  $\approx 200\mu m > \approx$  beam spot size

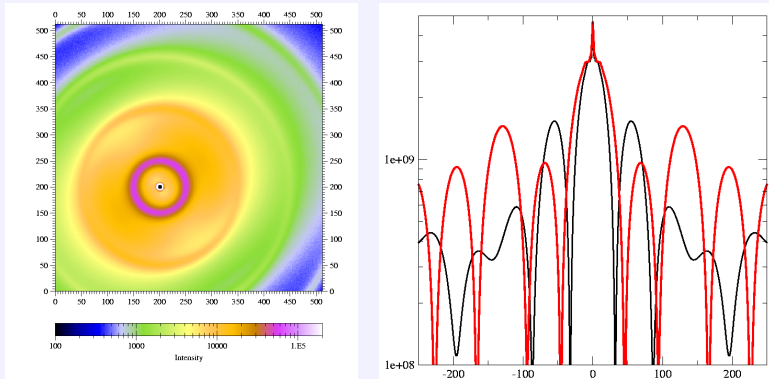
- detector has to be fixed on goniometer arm ⇒ mass, connection

**XPAD project (BM02.ESRF, IN2P3, CNRS-CEA)**

*Berar, JSR 2001, Boudet NIM-B 2004, Basolo IEEE-TNS 2005*

# Small Angle Scattering

Measure simultaneously data at low and high Q.

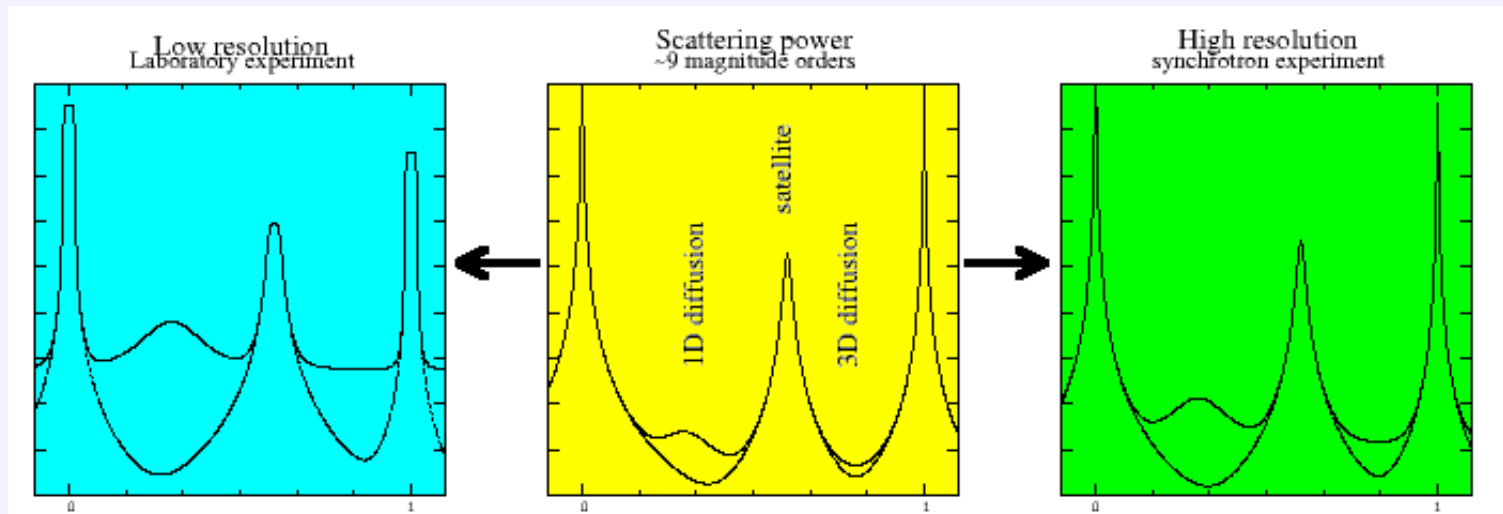


- 10 keV - 25 keV
  - $10^{-2}$  to  $10^8$  photons/s
- ⇒ 32 bits usefull
- small pixels needed around the beam stop

- Pixel size  $\approx 200\mu m > \approx$  beam spot size
- Real time acquisition with a frame time  $\approx 1ms$  and dead time  $< 1ms$
- The requirements are very similar to the previous ones and are a target in the XPAD project.

# New detectors, why ?

intensity	Bragg	Satellites	diffuse 1D	diffuse 3D
integrated	$N F^2$	$N_d N_c f^2$	$N = N_d N_c$	
maximum	$N^2 F^2$	$N_d N_c^2 f^2$	$N_d N_c^{5/3}$	$N_d N_c$

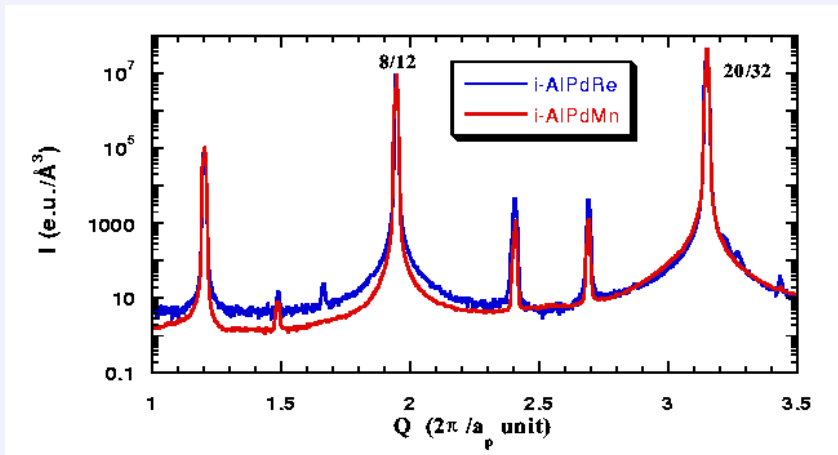


- ☞ Experimental resolution increases the required dynamic.
- ☞  $I_{Bragg} > 10^9 \nu/s$  (BM2@ESRF)  $\Rightarrow$  saturation ou atténuation.
- ☞  $F \propto \sqrt{I} \Rightarrow \sqrt{\text{dynamique}(I)}$ .

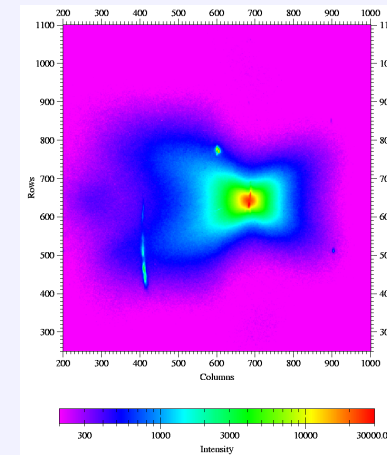
# On D2AM-CRG/ESRF beamline (BM2).

Very demanding experiments use slits and photomultipliers to reach the required quality.

In structural works, CCD cameras with indirect photon detection are commonly used.



Diffuse scattering in icosahedral quasi-crystals : 7 orders of magnitude are necessary to measure this signal. Dynamic extended by **attenuators**, time consuming mapping



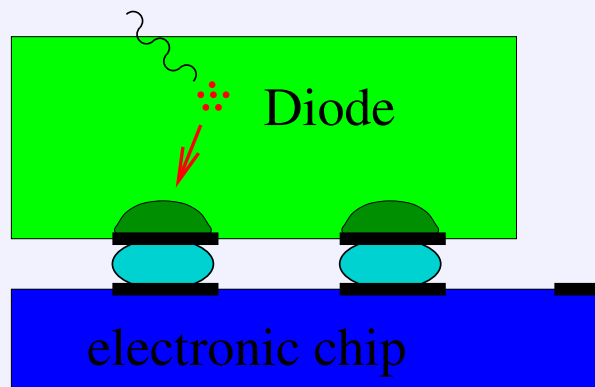
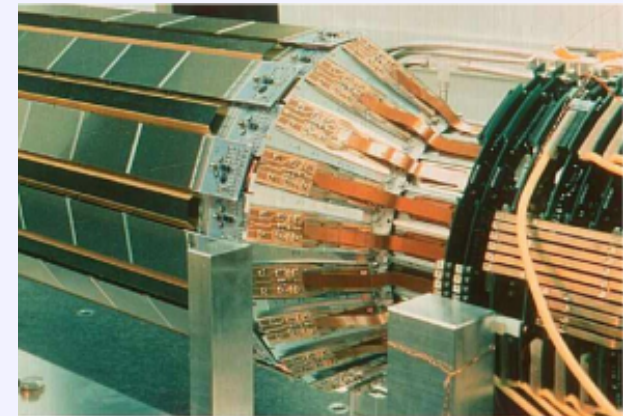
Complex shape of the diffusion around Bragg peak obtained by adding 10 (1000) frames. Out of peak to avoid blooming effects

Data from M. de Boissieu, see Phil. Mag. Let. (2001) 81, 273-283 and (2003) 83, 1-29

# D2AM-CRG/ESRF detector requirement

dynamic range	$> 10^9 \text{ count/pixel}$	$\Rightarrow 32 \text{ bits architecture}$
saturation rate	$> 10^7 \nu/s/pixel$	$\Rightarrow \text{noise} < 0.1 \nu/s/pixel$
energy range	$5 \rightarrow 25 \text{ keV}$	from beamline
pixel size	$250 \times 400 \mu\text{m}^2$	mean spot size in 1995
exposure time	$1 \text{ ms} \rightarrow 1000 \text{ s}$	kinetics potentiality

High energy physics experiments lead to built detector like Delphi at CERN which uses the potentiabilities offered by microelectronics and direct photon conversion in silicon.

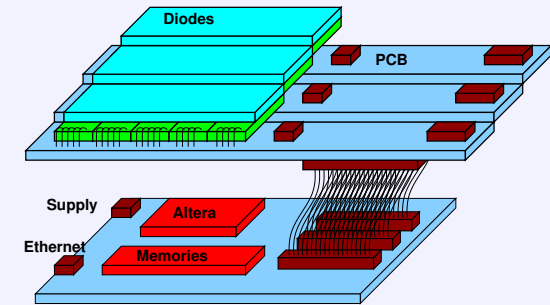
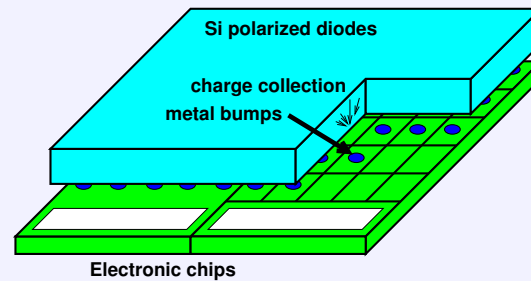


The silicium thickness  $300 \mu\text{m}$  and the pixel sizes  $330 \times 330 \mu\text{m}^2$  were convenient to our beamline requirements leading to the project of building a new X-ray detector taking benefit of the Delphi detector peoples knowledge.



# The XPAD project (XPAD1).

- Absorbed photons
- electron clouds
- charge migration
- electron bunches
- pixel threshold
- pixel counters
- on-board memories
- ethernet data

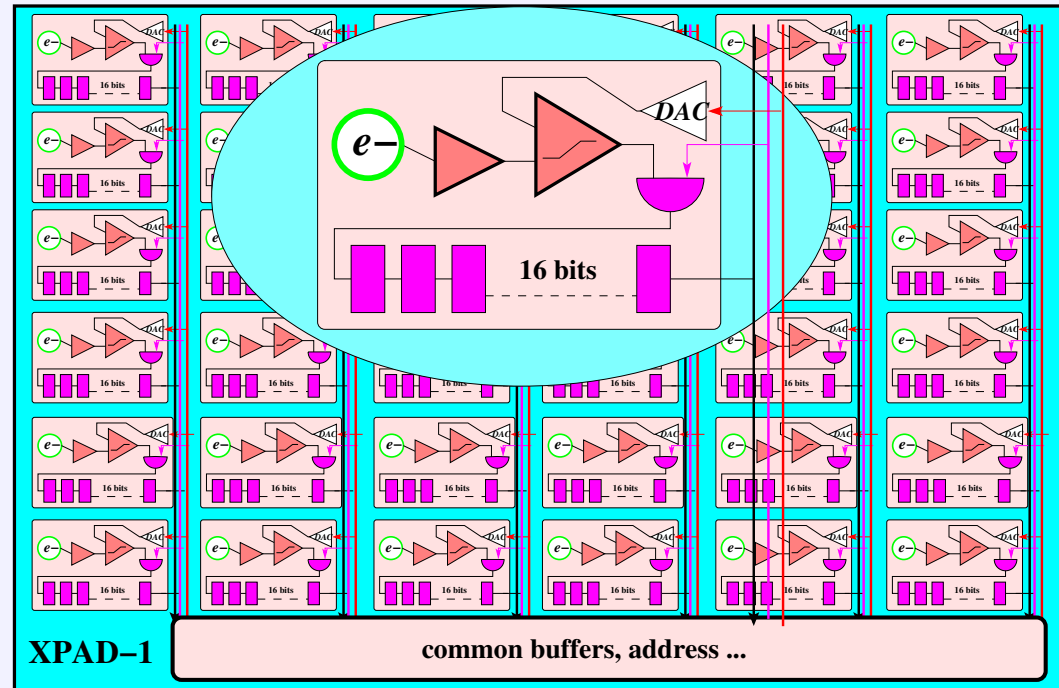


Diodes :

- high resistivity Si

Chips :

- AMS CMOS  $0.8 \mu m$
- $24 \times 25$  pixel/chip



Boudet *et al.*, NIM A510 (2003) 41-44,

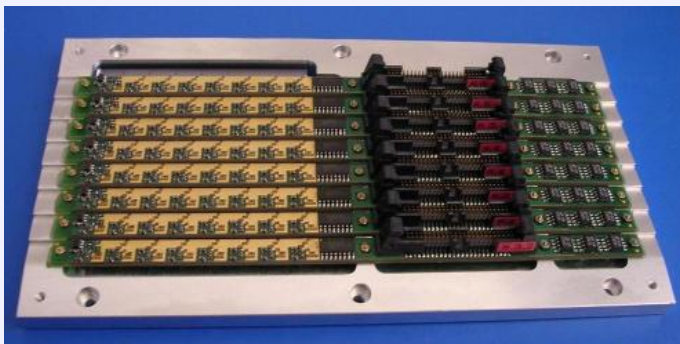
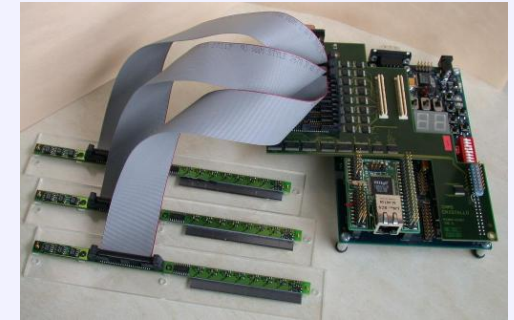
Berar *et al.*, J. Appl. Cryst. 35 (2002) 471-476

# XPAD2 detector : 8 modules $\times$ 8chips

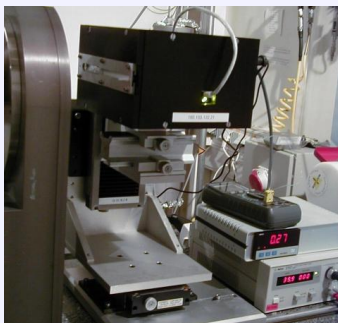
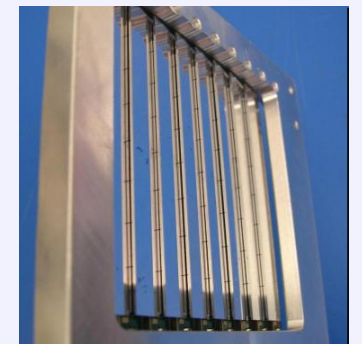
New diodes of  $500\mu\text{m}$  Si thick  $\rightarrow$  efficiency 78 % @15keV, 21% @25keV



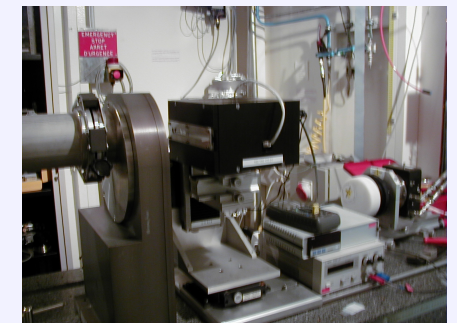
Diode  $\Rightarrow$  8 chips of  $24 \times 25$  pixels  
PCB card : drivers and regulators.  
Modules  $\Rightarrow$  acquisition card  
Altera Nios kit + ethernet



Tiled as close as possible  
 $\rightarrow$  reduce shading, dead zones.  
Metallic holder  $\rightarrow$  few  $\mu\text{m}$ .  
Size :  $200 \times 192$  pixels  
Surface  $\approx 68 \times 68\text{mm}^2$ .

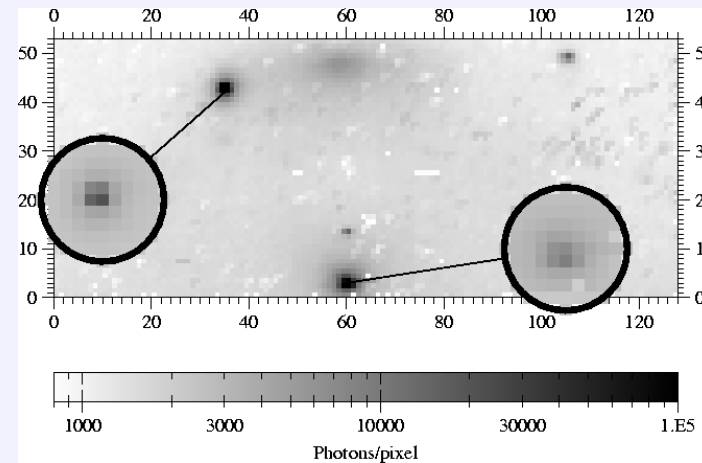
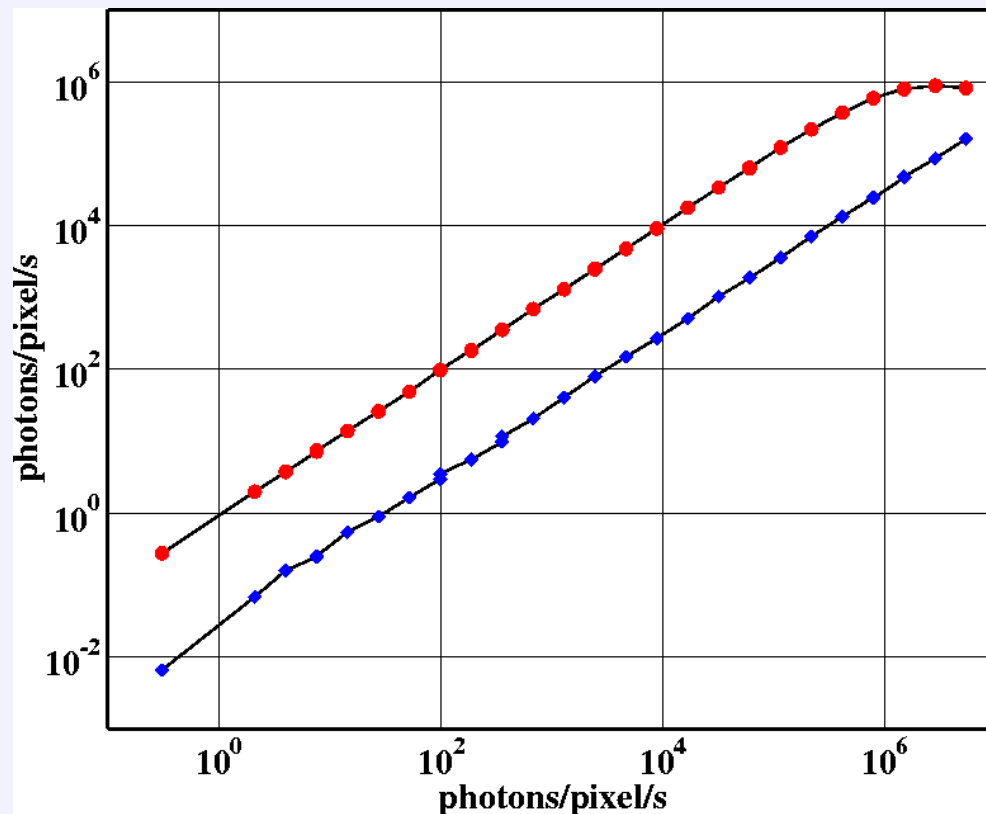


Interface software  
developed using LabWindows/CVI  
application software moves to Linux.  
XPAD prototype at SAXS station.

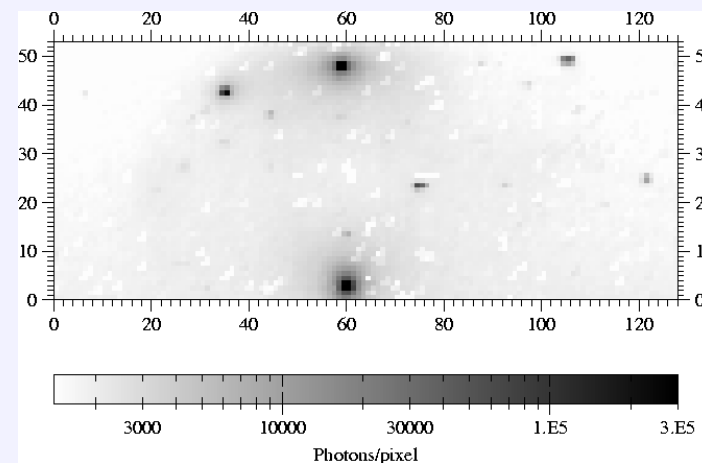


# Dynamical range (XPAD1)

The curves show the counts in two adjacent pixels as a function of the incoming flux on the more exposed pixel using XPAD chips.

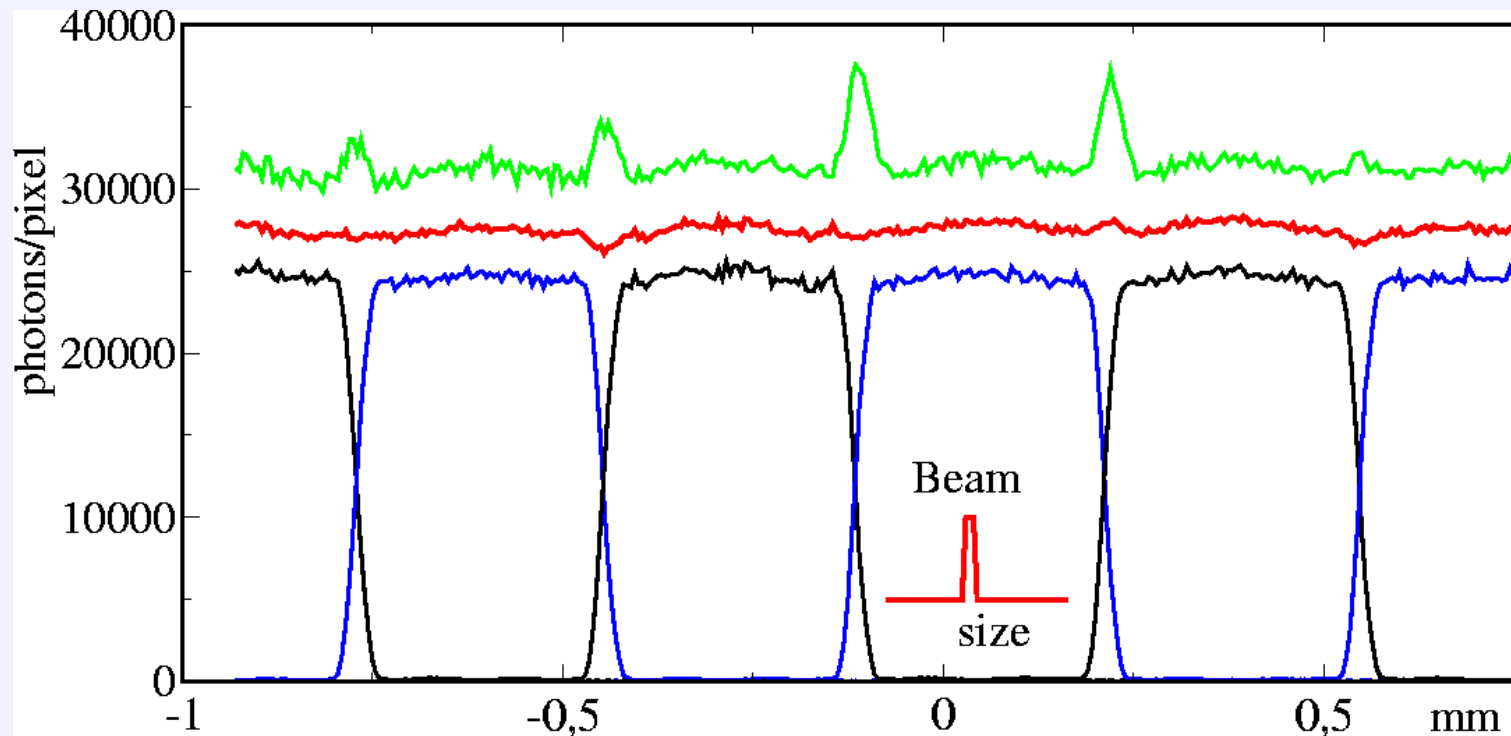


Diffusion (above) of a CdYb icosahedral quasicrystal and associated rotation image (below).



# Spatial resolution

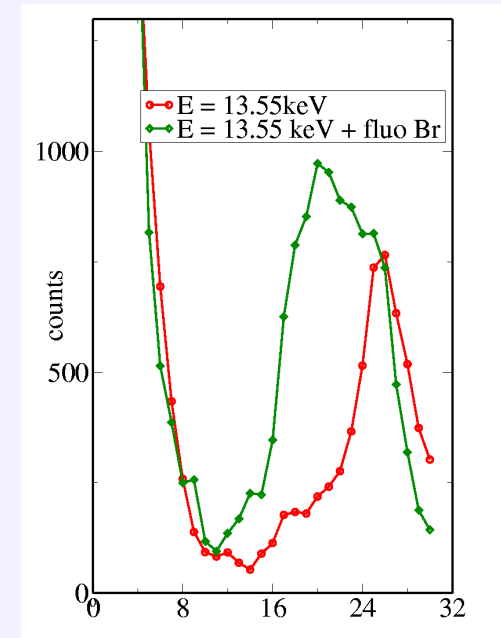
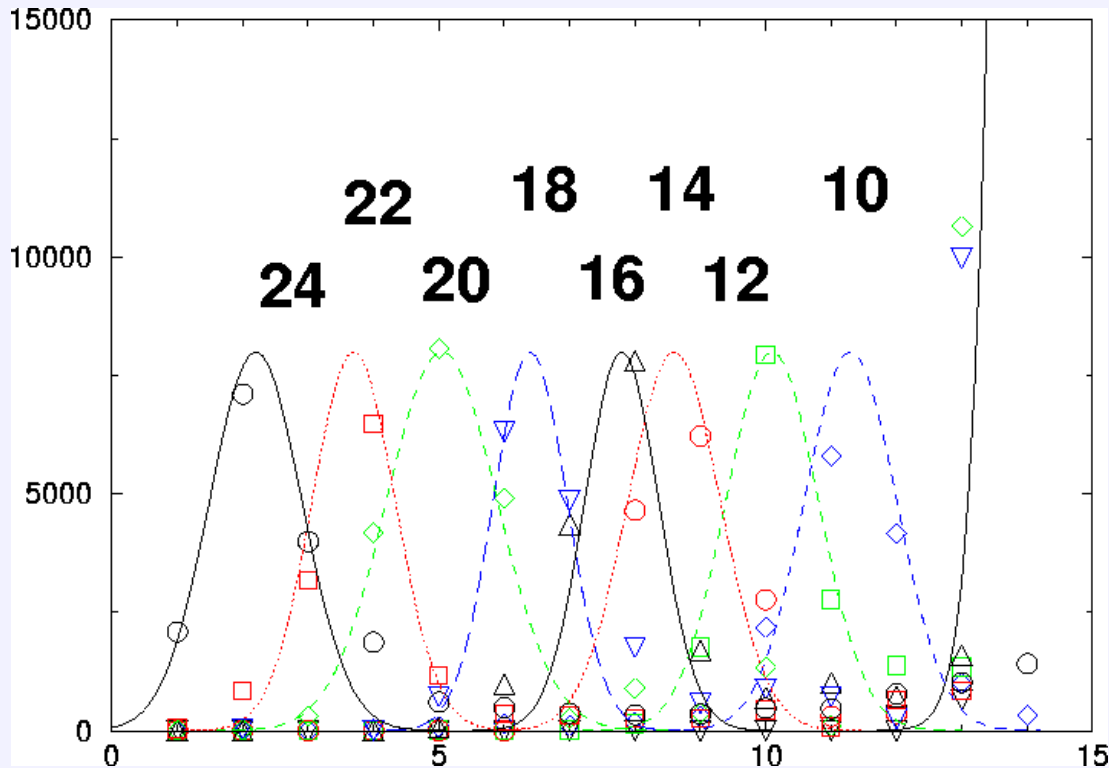
As the diode is common to pixels belonging to the same chip, some charge sharing may occurs between adjacent pixels. Measurements show that the charge sharing occurs on  $\approx 60 \mu m$ . This effect is a **physical limitation of pixel size** associated with absorption process. There is no significative influence of the bias field in the diode.



A flat field can be obtained when energies edge is perfectly adjusted in each pixel (red). In case of too low edges, this share sharing create some overcounting at pixel borders (green).

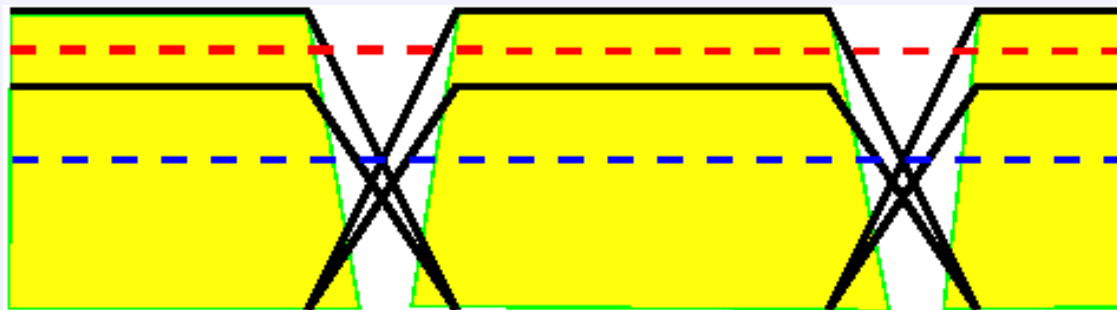
# Energy resolution

The conversion of incoming photons in silicon leads to a charge proportional to the incoming energy. The XPAD chip energy resolution is near  $1\text{ keV}$ .



Measured counts as a function of the threshold for the diffusion in of a Br solution on both sides of Br absorption edge.

## Energy resolution versus flat pixel detectors



- **Removing fluorescence**

Due to charge sharing on pixel borders rejecting  $E - 1keV$  create dead zones on this border with size  $d \approx 60\mu m$  : the flatfield will look like the yellow surface.

$\Rightarrow$  restricted to pixel size  $D > d$  : dead area  $\propto 2d/D$

- **Removing harmonics** needs a energy window with upper edge

More complicated :  $2E$  photons in the border zone are counted as  $E$  photons

Ratio reduced only by  $\propto d/D \Rightarrow$  **optics are more efficient!**



# Kinetics : low resolution powders

Very quick reactions, for solid state scientists, do not require such a high resolution but more flux and better detectors.

- Laser melting and solidification of oxides.
- Magnetic induction melting and solidification of metals.
- Self-Propagating High-Temperature Synthesis of alloys.

These systems are badly triggered and memory buffers must ensure to record the short phenomenon, most transformations occur in  $\approx 100 \text{ ms}$  but the whole process takes a few seconds ( $\approx 10 \text{ s}$ ).

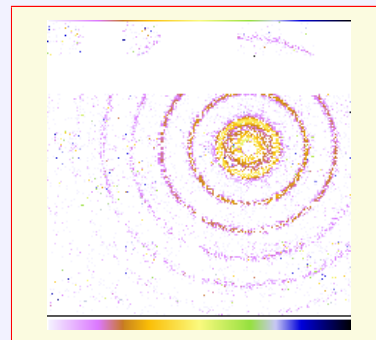
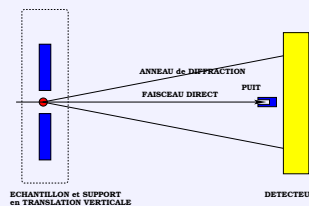
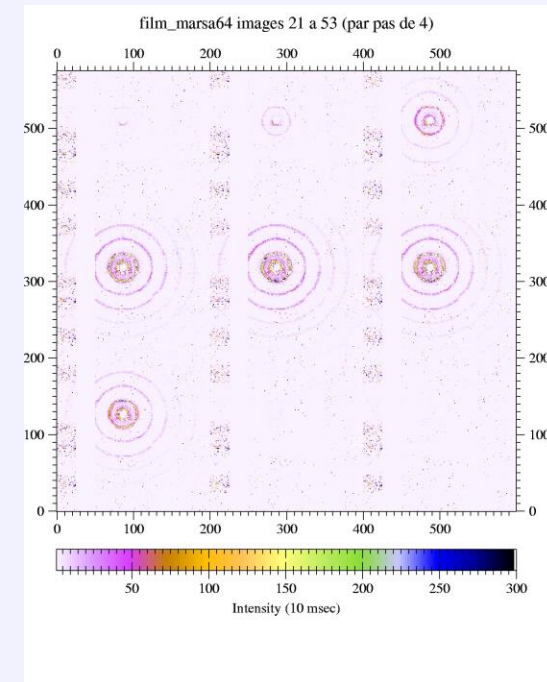
To study such phases diagram, various setups can be considered.

- Moving films (IP) are often too slow.
- Gas detectors with dedicated acquisition electronics (256 frames of 10 ms, no read out time) : limited detector counting rate (JF Javel, Thesis, Nancy 1998)
- X-Ray Intensifier and Frelon CCD camera (25ms frames but readout time 110ms/frame) : (C. Curfs, Thesis 2002, ID11  $2 \cdot 10^{12} \nu/s$ )
- Pixel or strip detectors : the way to succes if they reach the angular apperture needed, limited by windows of cell and the prototype number of pixels.
- ...

# Kinetics potentiality of XPAD2

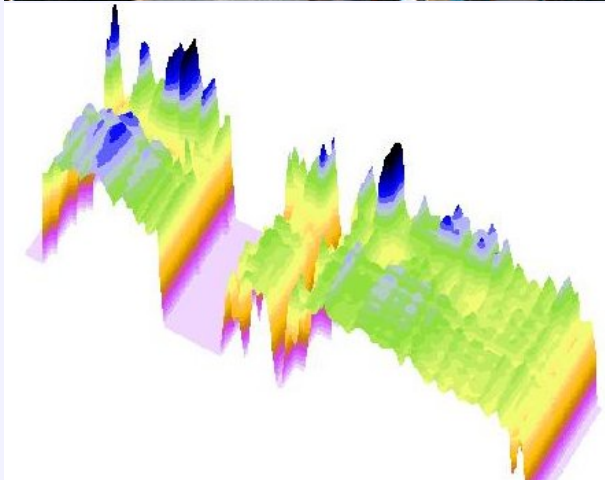
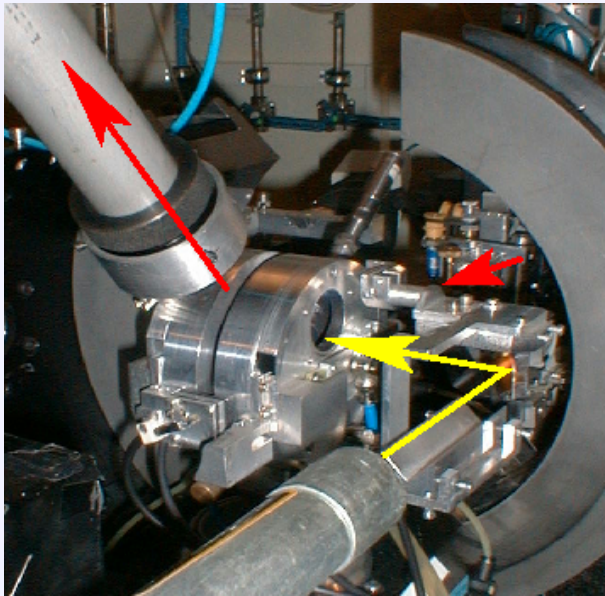
Whole electronic designed to allow kinetics studies (ms range)

- chips register 16bits + overflow
- on-board memories 32 bits
- exposure time :  $1ms \rightarrow 8300s$
- dead time for reading :
  - whole image  $2ms$
  - overflow  $16\mu s$  each  $10ms$
- on-board storage :
  - 423 images  $< 10ms$
  - 233 images  $\geq 10ms$

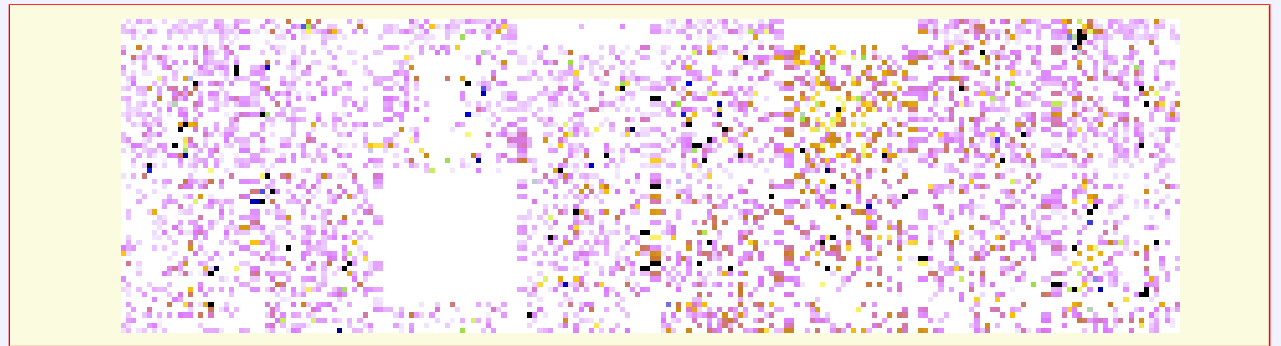


Images of 10 ms each taken off a 2s movies showing diffraction while the sample crosses the beam at D2AM SAXS camera.

# Kinetics of quench studied by diffraction



Data collection is limited by the cell aperture, which has been designed for linear detector, a few frames of 20ms around crystallisation shown at 10 frames/s during  $\text{CaAl}_4\text{O}_7$  quench.

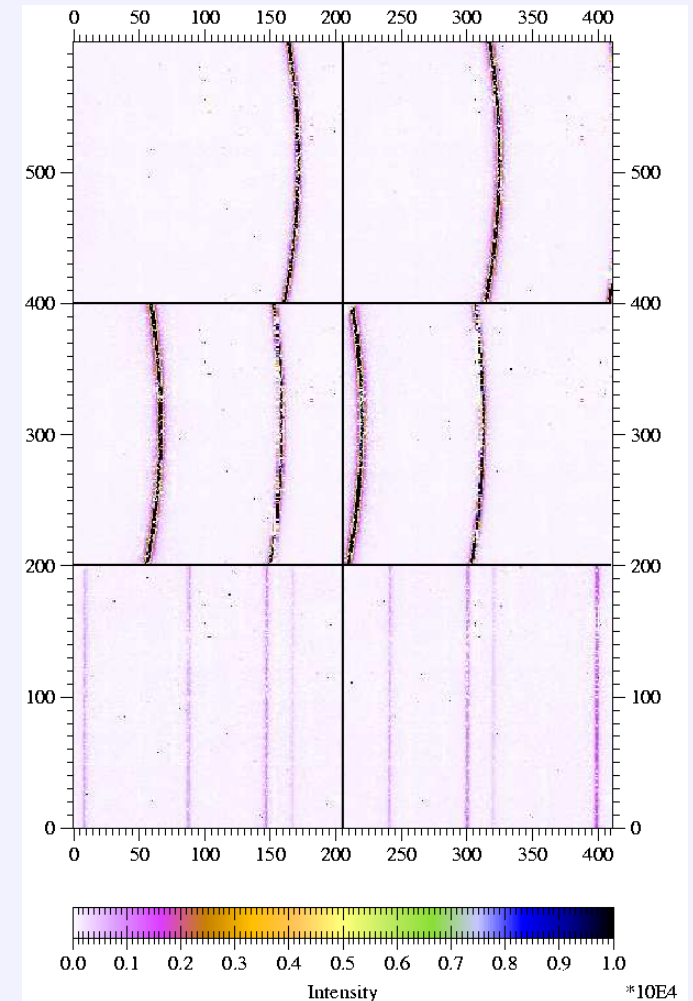
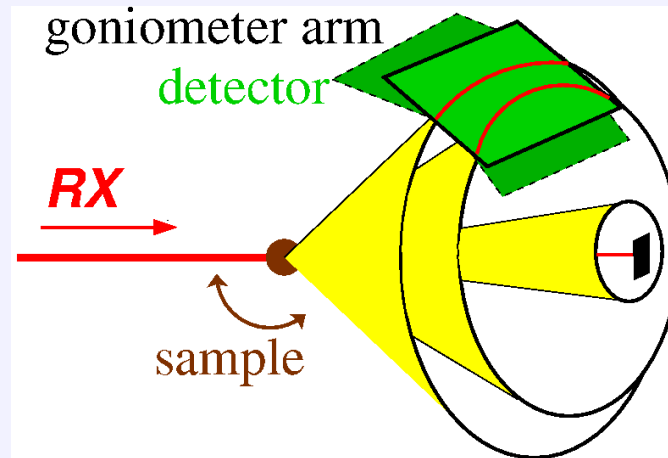
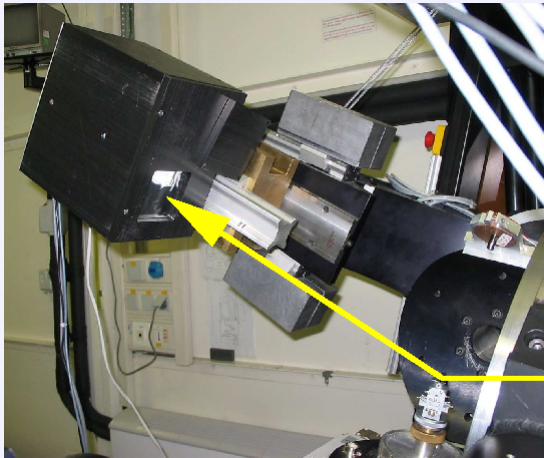


The quench of  $\text{Al}_{2x}\text{Ca}_y\text{O}_{3x+y}$  ceramics can lead to vitreous or crystalline oxides. The transition between the liquid state and the crystalline one occurs in less than 20ms and may exhibit some transient phases.

# Powder diffraction application (1)

Scintillator and slits → 2d-detector.

- Diffraction along cones
- Data redundancy with 2D detector
- $60^\circ$  collected at high resolution
- angular apperture  $4^\circ$  at  $1m$



With 0-D detector pipes remove diffuse scattering, background level partly removed with conic pipes on 2d-detector.

Raw images with Bragg lines, low and high angles.



# Powder diffraction application (2)

Resulting counts  $Y$  on pixel  $p$  :  $Y_p = N_p^{-1} \sum f_q y_{q,i}$   
 $y_{q,i}$  counts on image  $i$  of pixel  $q$ ,  
 $f_q$  flatfield of pixel  $q$  :

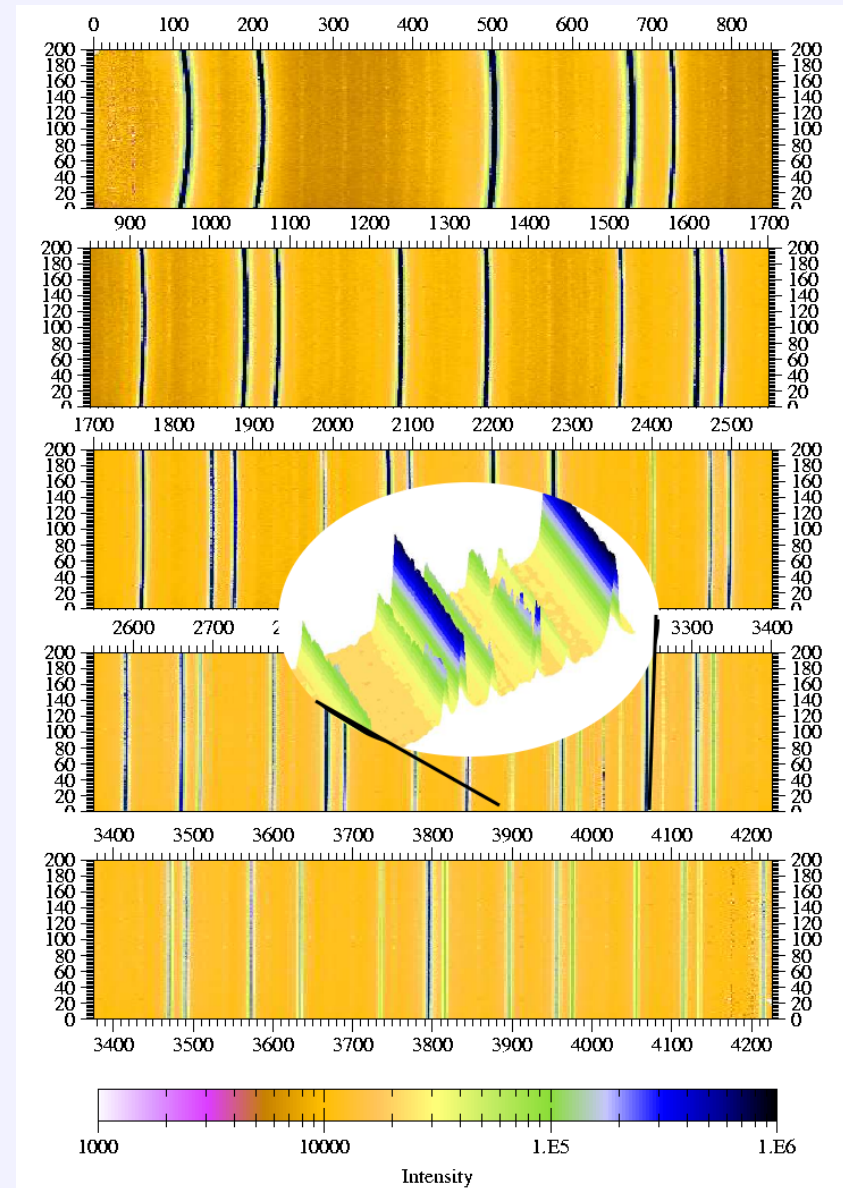
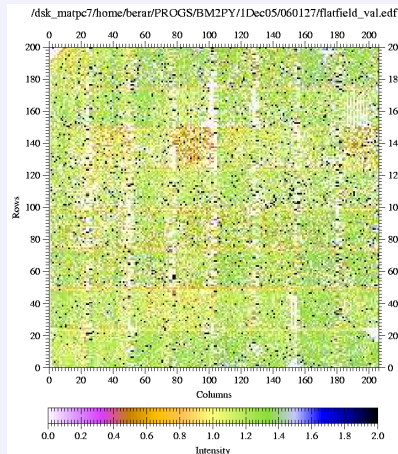
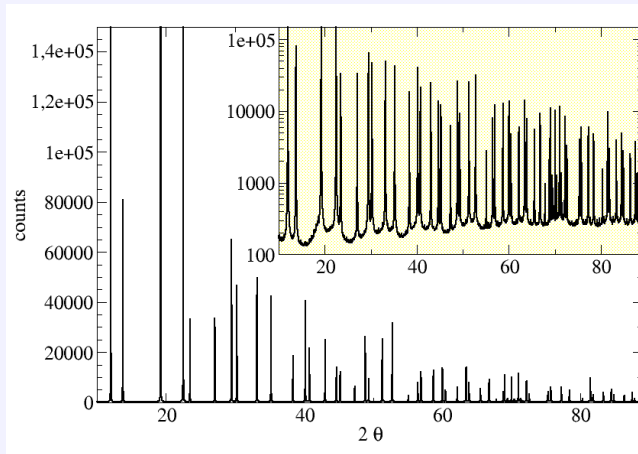
Pixel :  $q \in Image_i \rightarrow p \in Image_{merged} : q = q(p, i)$

Minimisation:  $\sum_p (Y_p - N_p^{-1} \sum_i f_q y_{q,i})^2$

Powder lines :  $Y_{p \in Ring} \rightarrow Y_{Ring}$

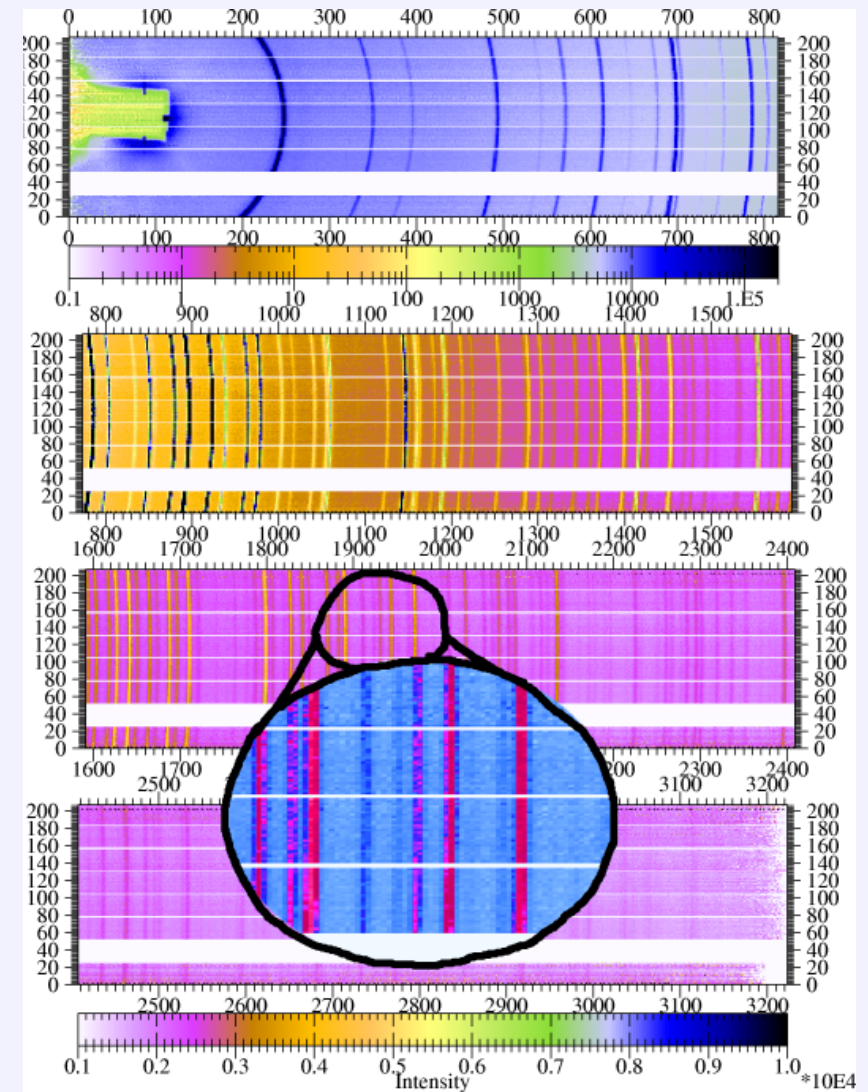
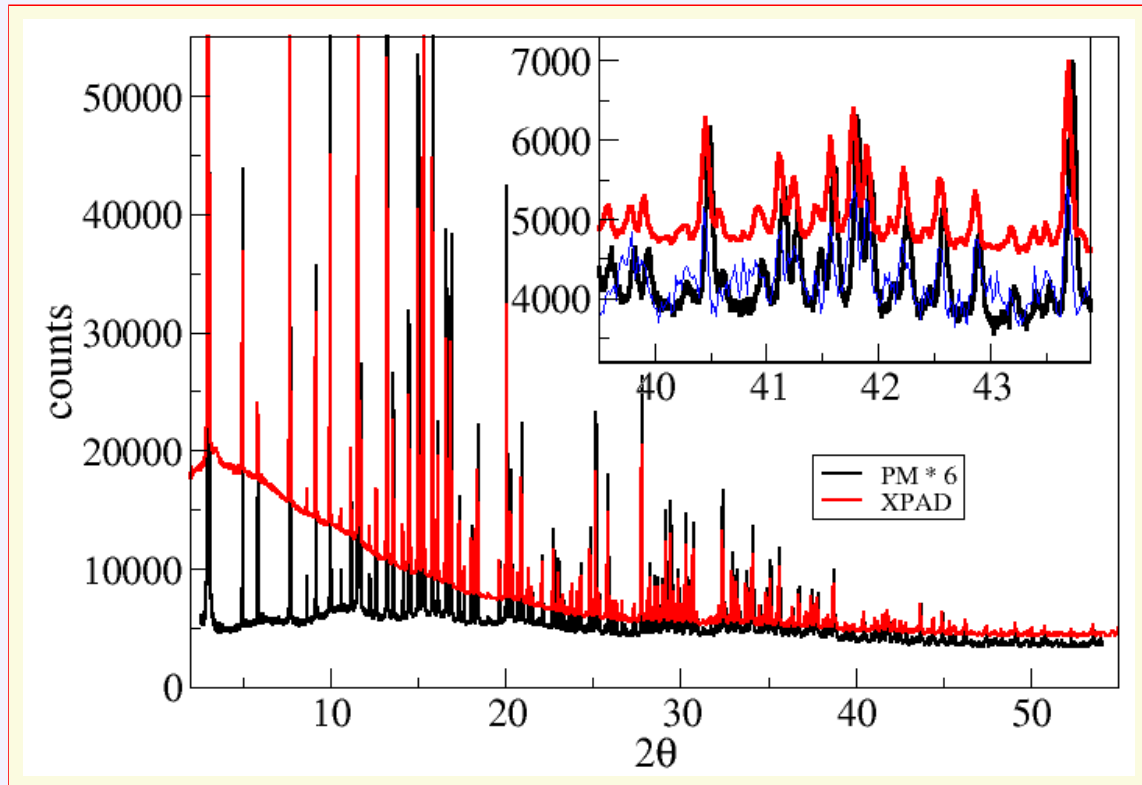
$$\sum_{Ring} (Y_{Ring} - N_{Ring}^{-1} \sum_{p \in Ring} \sum_i f_q y_{q,i})^2$$

- Reconstructed Debye-Scherrer film  $\rightarrow$
- Powder diagram + flatfield extraction



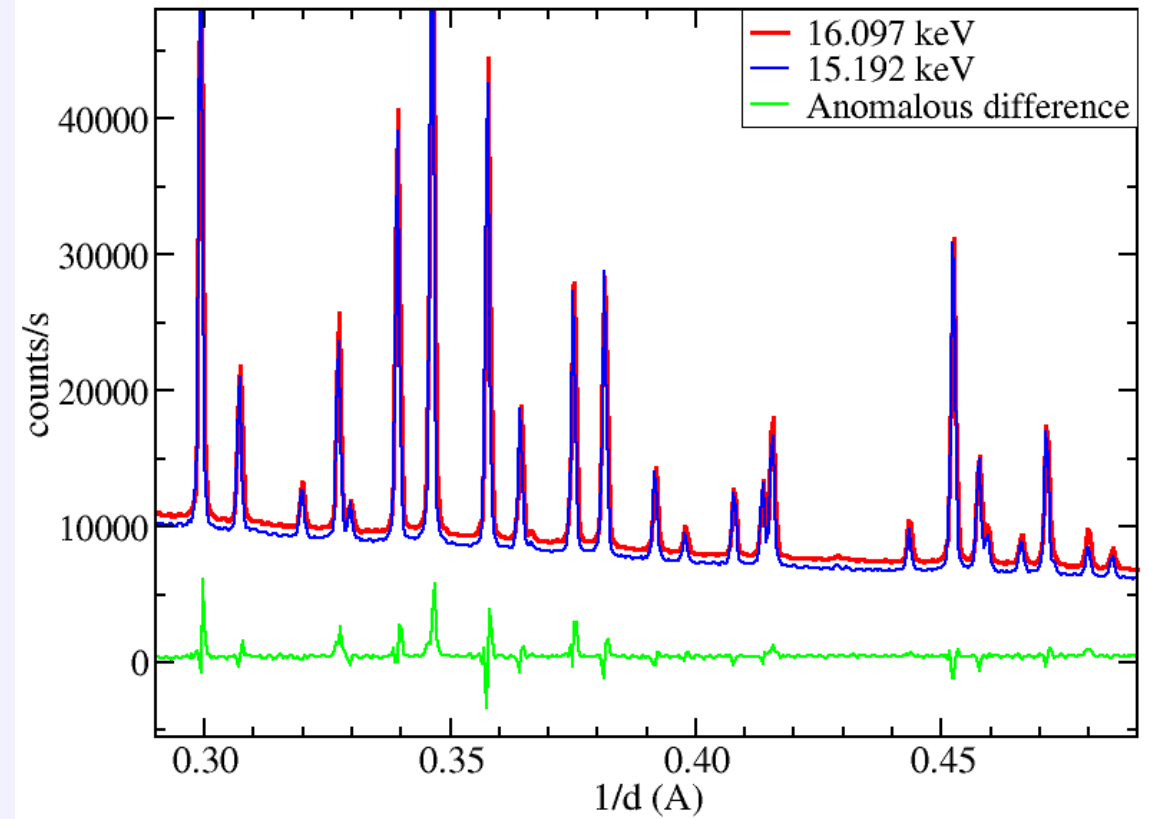
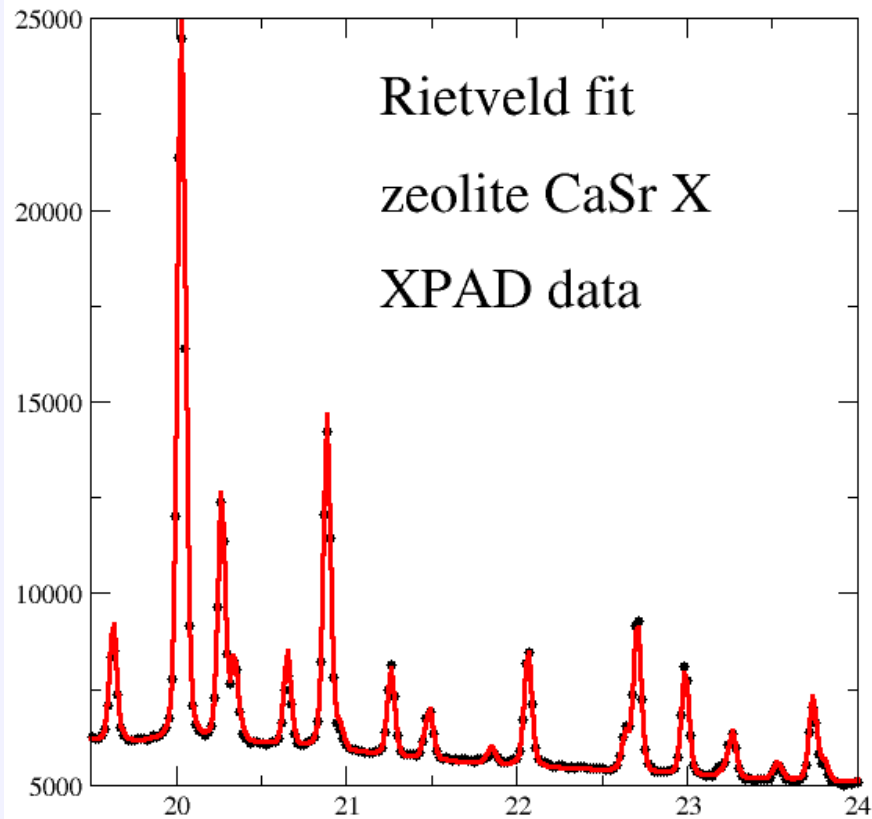
# Powder diffraction application (3)

- Can be applied to complex materials : Zeolite
- High quality powder pattern can be extracted with time reduced by 20.





# Powder diffraction application (4)



Rietveld method :  $R_{wp}=8.8\%$

$R_{exp}=4.1\%$  and  $R_{bragg}=4.4\%$

Atomic parameters same as conventional

Whole experiment time  $\rightarrow 1/20$ .

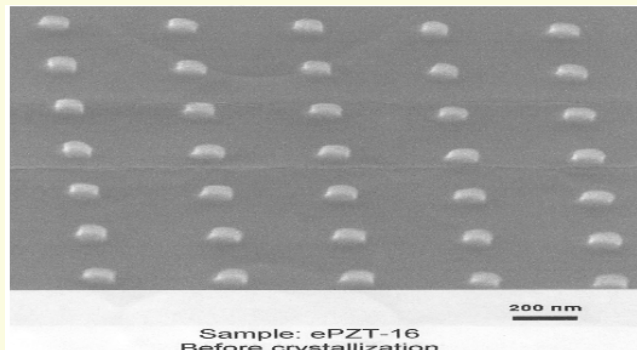
Data quality allow the use of anomalous difference.

Data recorded in 1/200 time will lead to similar results.

# Multilayers

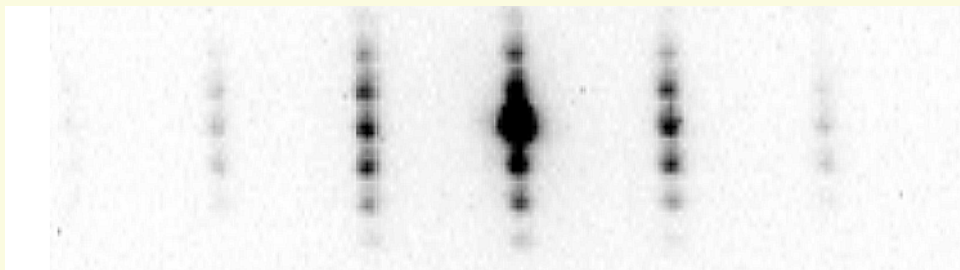
Challenging applications on material science beamlines consist in :

- **anomalous mapping** of layered materials
- **local structure** of self organized layers (Qdots...)

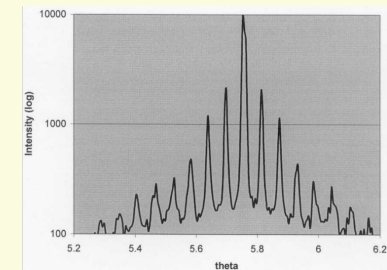


Ferroelectric  $\text{PbZrTiO}_3$  dots  
size = 80 – 100  $\text{nm}$   
spacing = 300  $\text{nm}$   
coverage area =  $0.4 \times 0.4 \text{ mm}^2$ .

Diffraction imaging is a non destructive study.



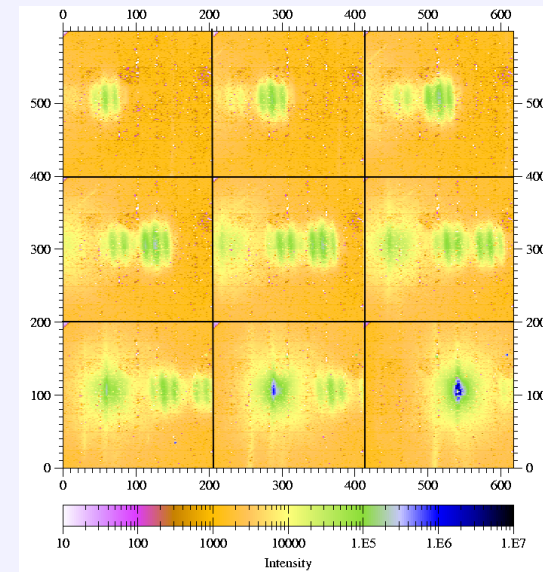
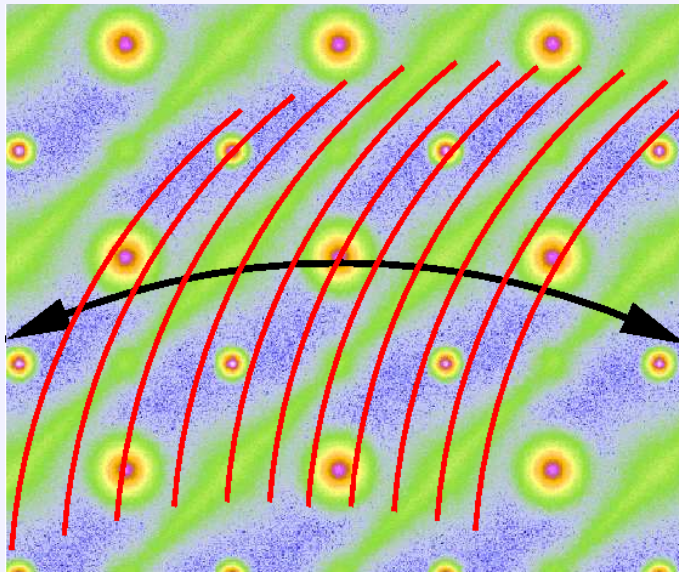
CCD / Counter



Pixel detector is required to reach the needed data quality.

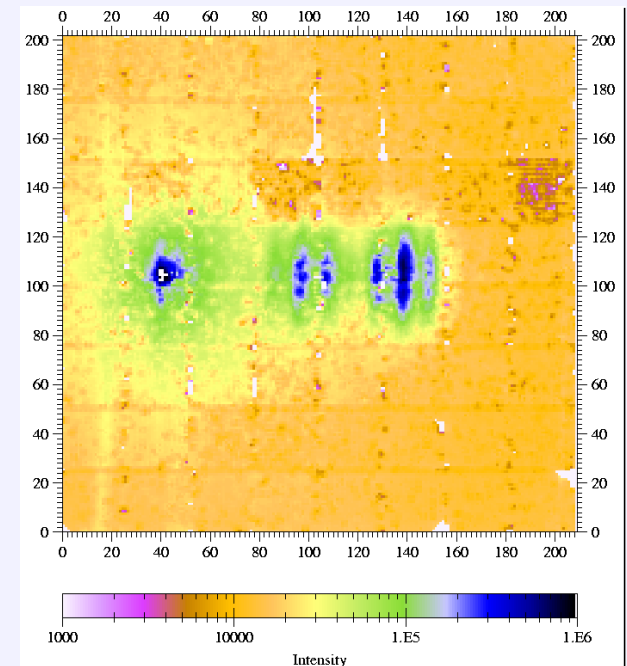
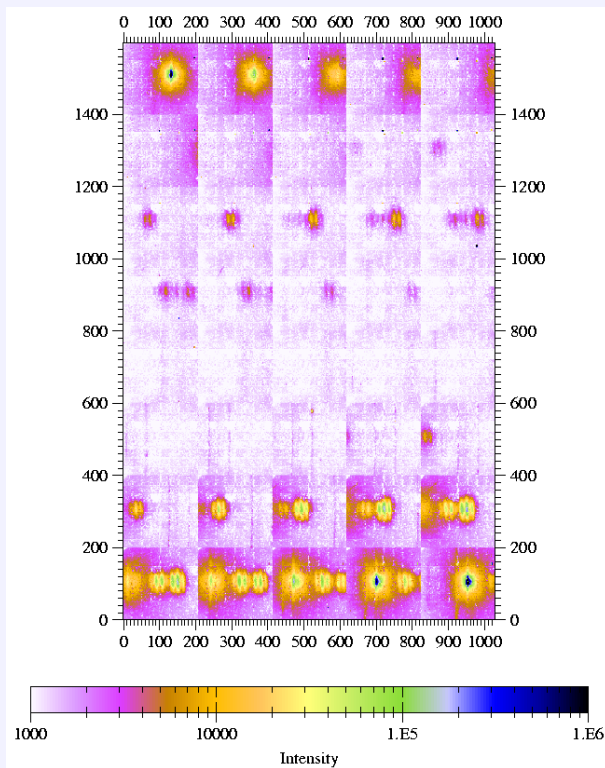
# Multilayers measurements

Epitaxially grown multilayers are now common samples to characterize: they need mapping of the reciprocal space which is time consuming. At the time such maps are recorded with slits and fixed  $(h, k, l)$  point of the reciprocal lattice, attenuators are often required near the substrate. 2-D detection allows an important improvement in these acquisitions but it needs to be able to manage high dynamics and to transform your reciprocal slices into reciprocal maps.



# Multilayers slice / integration

A PBT superlattice / MgO has been scanned along the  $(00l)$  direction. Images of 200s have been recorded from 5.95 to 4.05 with a  $l$  step of 0.05, these was preferred to direct integration of this space as it allows to measure more accurately the shape of the lower peaks.

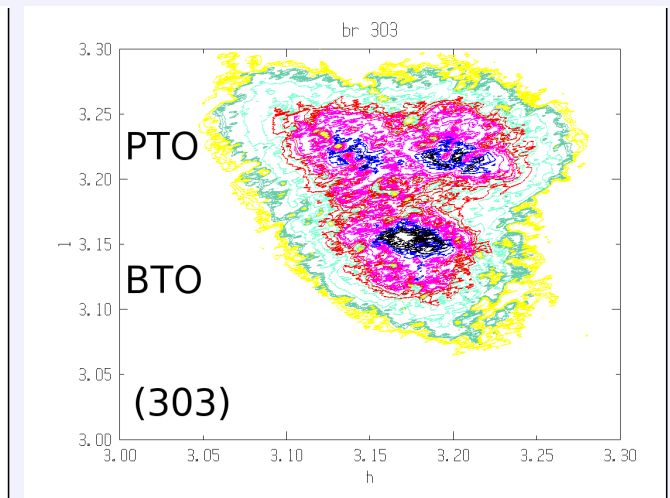
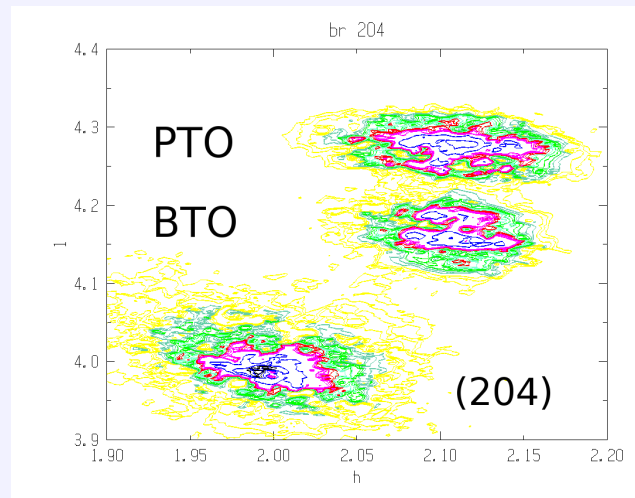
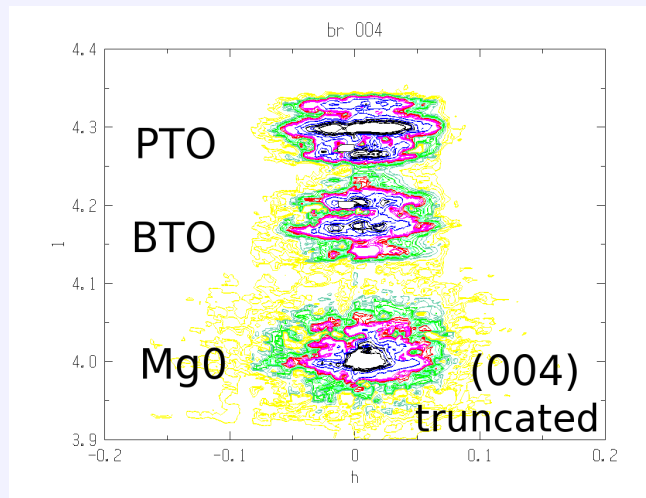




# Multilayers ; Ferroelectric superlattice

27 (17 PbTiO<sub>3</sub>,17 BaTiO<sub>3</sub>) superlattice / MgO :  
large lattice mismatch → in-plane polarization → tetragonal distortion.

Physical behaviour of such compounds is primarily dependent on their epitaxial crystalline quality, their composition and their structural perfection.



Out of plane : strain / chemical

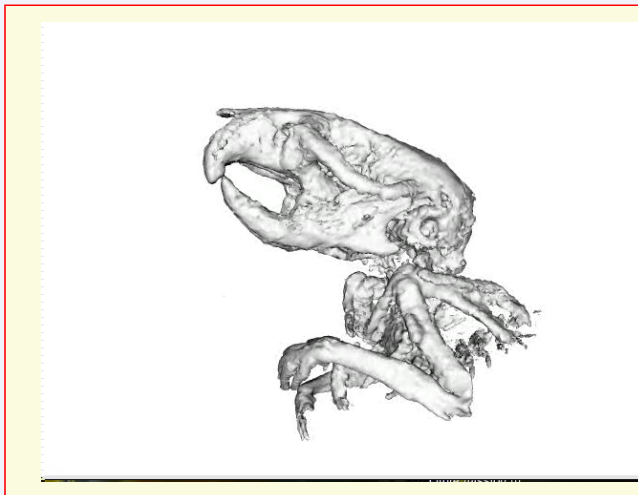
In plane : 2 PTO domains tetragonal distortion

The reciprocal maps are recorded scanning the XPAD detector and rebuilt from the collected reciprocal slices. Compared to standard data collection the time can be reduced by 100. Intensity on substrate peak can reach  $10^9 \nu/s$  !

F. Lemarrec, E. Dooryhee and coll., IUCr (2005) Florence, Italy

# A new detector using last XPAD2 chips.

- The detector build in winter 2004 has some defects and few chips were damaged by some experiments.
- A new one was assembled using spare chips and best remaining modules. It was mainly used for the small animal tomography project.



**Small animal tomography** : few frames (18/72) from a mouse rotated in laboratory Xray beam and the 3D reconstruction of the bones by tomography. Note that all chips have been repaired and no more defects can be evidenced.

project in collaboration with R. Khouri, C. Morel, F. Peyrin, D. Sappey-Marini er, S. Valton...



# CCDs compared to hybrid pixels

	direct CCD	FO CCD	XPAD2
X ray detector	silicium $20\mu m$	fluo screen $50\mu m$	silicium $330\mu m$
coupling		optical (+intens)	electric
$1\nu @ 10keV$	$3000e^-$	$1 - 5e^-$	$3000e^-$
saturation	$10^2\nu$	$10^5\nu$	
Energy resol.	10%		10%
Read	90% dead time	$\approx 1s$	$\approx 0.01s$
Flux Max	$10^4\nu/s/detector$		$10^6\nu/s/pixel$
Shutter	X	X/optical	integrated
Dynamic		14-16b	
Sensitivity	$0.001\nu/s/pixel$	$0.5\nu/s/pixel$	$0.01\nu/s/pixel$
Measurement	counting	Integration	counting
Limitations		dark removing blooming effect	counting rate
Opt. usage	Speckle	Structure	Mat. Sciences

# from XPAD2 to XPAD3

- Obsolescence of the AMS-CMOS  $0.8 \mu m$  technology used for XPAD2
- A new XPAD3 using  $0.25 \mu m$  technology with  $25 \mu m$  bumps

	XPAD2	XPAD3	comments
polarization	both	$e^+$	2 chips : Si, CdTe
pixel size	$330 \mu m$	$130 \mu m$	
chip size	$8 \times 10 mm^2$	$10 \times 15 mm^2$	→ reduce tiling
counting rate	$2 \cdot 10^6 ph/s$	$2 \cdot 10^5 ph/s$	≡ count/surface
energy range	(5) $15 \rightarrow 25 keV$	$7 \rightarrow 25 keV$	new analog chain
pixels/chip	$24 \times 25 = 600$	$80 \times 120 \approx 1 \cdot 10^4$	
pixels/module	$8 \times 600 \approx 5 \cdot 10^3$	$\approx 1 \cdot 10^5$	
pixels/detector	$\approx 4 \cdot 10^4$	$\approx 5 \cdot 10^5$	
geometries	$8 \times 8$ or $2 \times 5$	$7 \times 8$ and ?	

- Chip design has been carried out
- Prototype is expected for mid 2006.